Reprinted from Preprint Volume: 18th Conference on Radar Meteorology, Mar. 28-31, 1978, Atlanta, Ga. Published by the American Meteorological Society, Boston, Mass.

DOPPLER RADAR MEASUREMENTS OF THE AIRFLOW WITHIN A MESOSCALE COLD-FRONTAL RAINBAND

Thomas J. Matejka and Robert A. Houze, Jr.

Department of Atmospheric Sciences
University of Washington
Seattle, Washington 98195

1. INTRODUCTION

Data from radars, analyzed alone or in conjunction with other types of meteorological information, have consistently shown that the precipitation in extratropical cyclones is often concentrated in mesoscale areas and bands (Browning, 1974; Harrold and Austin, 1974; Houze *et al.*, 1976a). The relationship of the mesoscale precipitation features to frontal structure and to synoptic and frontal air motions has been determined in case studies such as that of Houze *et al.* (1976b). In only a few studies, however, (e.g., Browning and Harrold, 1970; Browning *et al.*, 1973) has detailed information about the airflow within the mesoscale cloud features been obtained. Yet, such knowledge is essential to the understanding and modeling of the development of precipitation in mesoscale cloud features, and may well be crucial to understanding mesoscale frontal dynamics.

In this paper we present an analysis of the detailed airflow in a vertical cross-section through a mesoscale cold frontal band of precipitation. This flow pattern is based on data obtained with the National Center for Atmospheric Research's (NCAR) CP-3 Doppler radar during the autumn, 1976, observational period of the University of Washington's CYCLES (Cyclonic Extratropical Storms) PROJECT.[1]

2. DATA

The CP-3 Doppler radar has been described by Gray *et al.* (1975). It has a wavelength of 5.45 cm, beamwidth of 1°, and peak power of 338 kW. The radar is instrumented with a pulse-pair processor (Lhermitte, 1972; Groginsky, 1972) which determines the mean velocity along the radar beam of precipitation particles at the same time that their reflectivity is measured. In this study, the mean reflectivity and velocity were recorded in range bins 0.27 km in width and at azimuth intervals of 1°. The CP-3 radar is equipped with a color-display which is particularly well-suited for indicating wind and divergence patterns in extratropical cyclonic storms (Baynton *et al.*, 1977).

The CP-3 radar, which was located at Pt. Brown, Washington (Fig. 1), was operated in a three-dimensional scanning sequence in which the antenna was rotated through 360° of azimuth at a sequence of fixed elevation angles: 0, 1, 2, 3, 4, 5, 6, 7, 11, 15 and 19°. A three-dimensional scan was obtained once every 30 min, and the vertical cross sections presented in this paper have been constructed from these basic scans.

The CYCLES PROJECT also includes the operation of the University of Washington's B-23 research aircraft, the NCAR Sabreliner aircraft, two University of Washington research radars inland in Seattle, serial rawinsondes, and a network of high-resolution rain gauges and surface instruments across southwestern Washington. In this paper, however, we focus on the air motions revealed by the CP-3 radar. Detailed surface records of pressure, temperature, wind velocity, and rainfall rate obtained at the radar site are also referred to, as is cloud imagery from the SMS-2 weather satellite.

3. REFLECTIVITY PATTERN OF THE COLD FRONTAL PRECIPITATION

On 17 November, 1976, a cold front moved east-southeastward into Washington State. The front was associated with an occluding extratropical cyclone centered 1200 km to the north (Fig. 1).

The frontal passage at the surface at the radar site occured at 0730[2] and was marked by a rise in pressure, a slight drop in temperature, and a shift in the wind from 220° at 9 m s^{-1} to 275° at 6 m s^{-1} within 10 min. The windshift accompanying the frontal passage appeared as a marked line of discontinuity in the velocity field on PPI color-displays of the CP-3 radar. This line of discontinuity could be tracked and was used to indicate the progress and orientation of the surface front as it moved across the area covered by radar.

Reflectivity measurements obtained with the CP-3 radar showed that the precipitation associated with the cold front consisted of a large mesoscale band, 110 km in width, along the cold front; this band is depicted in Fig. 1. Some mesoscale bands and areas of precipitation in the warm sector of the cyclone immediately preceded the cold-frontal band.

A vertical cross-section of reflectivity through all but the leading edge of the cold-frontal band is shown in Fig. 2. The position of the cold front sketched onto this and subsequent figures was determined by the top of the layer of cold advection, as indicated by the backing of winds with height, and by the position of the surface windshift line.

[1]The CYCLES PROJECT is conducted by the Cloud Physics Group, Prof. Peter V. Hobbs, Director, Department of Atmospheric Sciences, University of Washington.

[2]All times are Pacific Standard Time (PST).

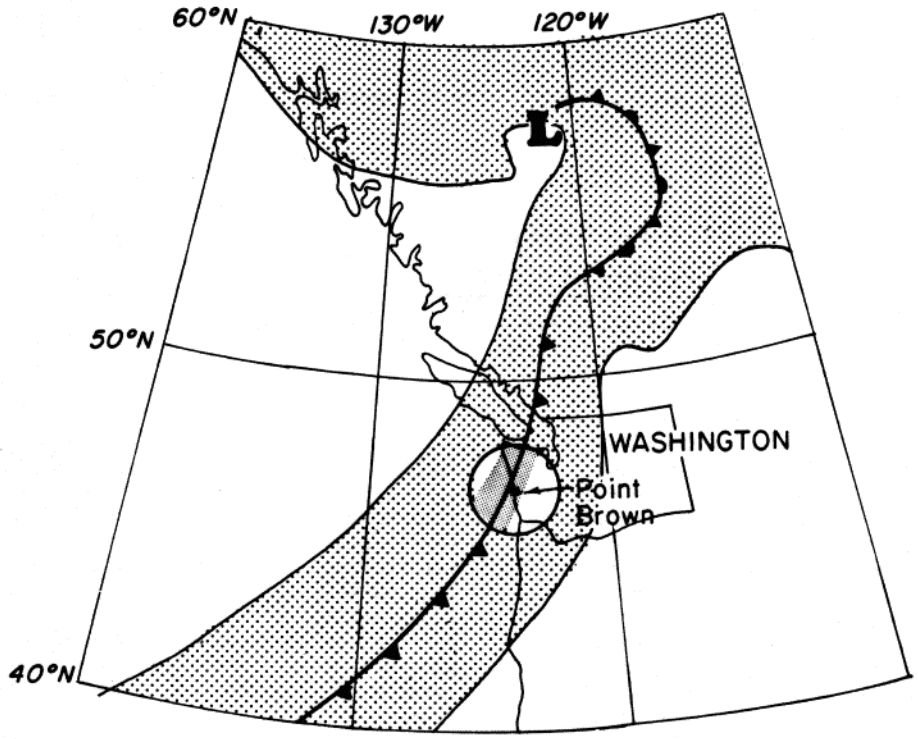

Figure 1: Location of the NCAR CP-3 radar at Point Brown, Washington, and its area of coverage (circle). Also shown are the cloud shield (light shading), the large mesoscale cold-frontal band seen with the radar (dark shading), and the surface positions of the front and center of low pressure at 0715 PST.

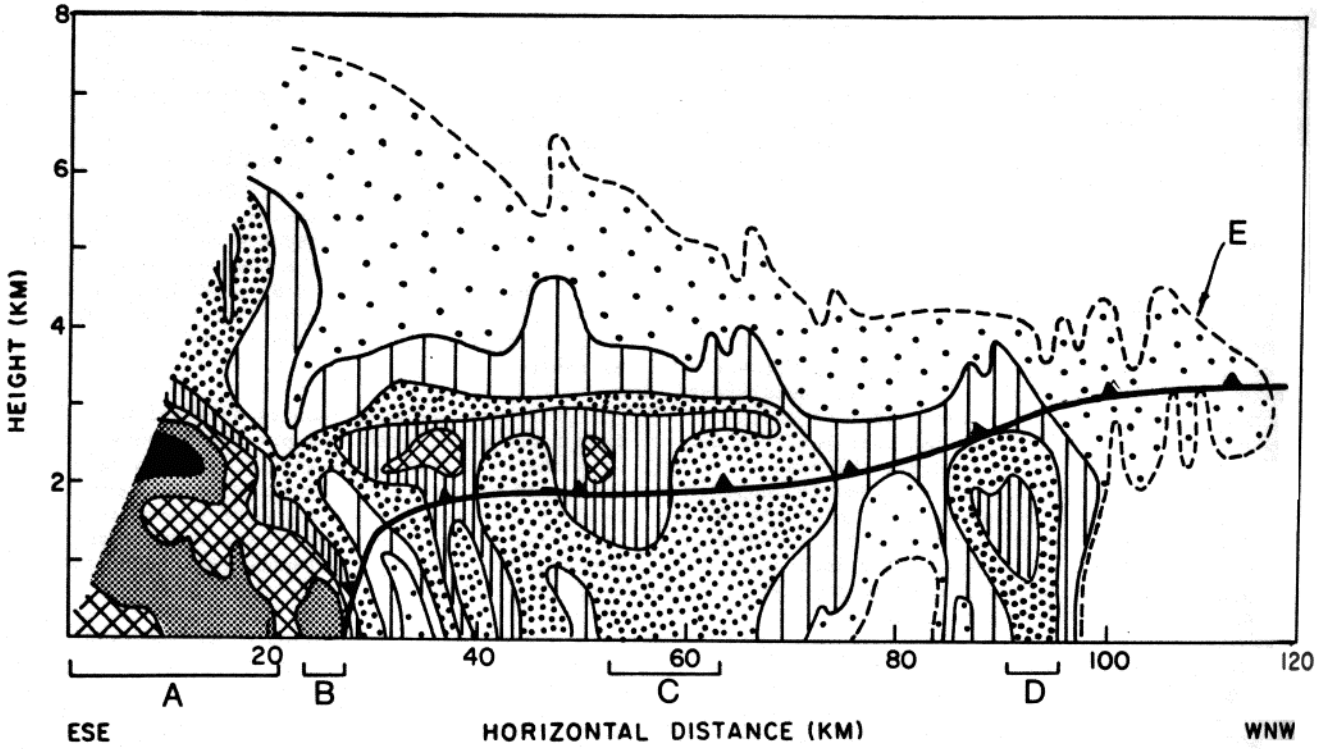

Figure 2: Cross-section of reflectivity through the mesoscale cold-frontal band at 0700 PST. The radar site corresponds to the left edge of the figure, and distance to the right represents distance toward the west-northwest, along an azimuth of 294° from the radar. The outermost contour is the boundary of the minimum-detectable echo; inner contours are 17, 22, 27, 32, 37, and 42 dbz. Letters are referred to in the text.

The large mesoscale cold-frontal band itself contained several smaller mesoscale sub-bands of higher reflectivity, all oriented roughly parallel to the larger band. The strongest and most distinct of these was 25 km in width and located toward the leading edge of the cold-frontal band. Most of this sub-band appears in Fig. 2 as the area of high reflectivities indicated by letter A. The surface cold front was located to the rear of this sub-band and was accompanied by a thin, broken line, approximately 4 km in width, of intense, cellular echoes (Letter B in Fig. 2 indicates one of the cells.) Additional, weaker sub-bands of precipitation within the large mesoscale cold-frontal band followed the frontal passage (C and D in Fig. 2). The precipitation rate increased as they passed; the general tendency, however, was for the precipitation rate to taper off after the frontal passage, stopping altogether at 0908 as the back edge of the cold frontal band passed through. Precipitation aloft (E in Fig. 2) continued behind the back edge of the band of rain at the surface, but evaporated before reaching the surface.

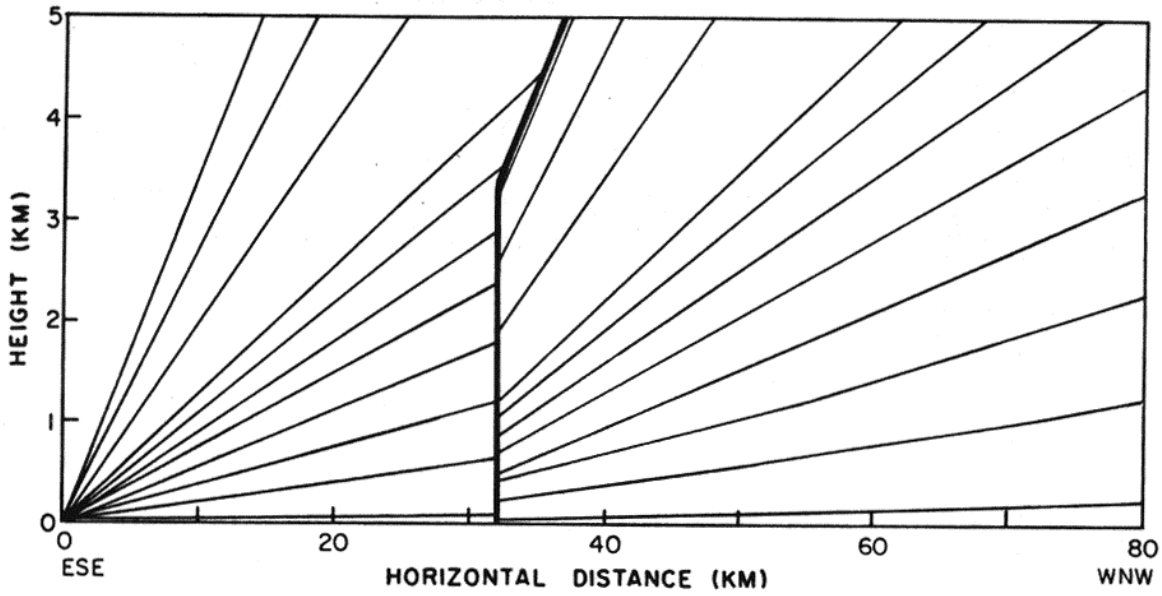

Figure 3: Cross-section through the mesoscale cold-frontal band showing the rays of data available for the construction of the cross-sections in Figs. 4-6, in which the left portions are based on data from 0700 PST, the right from 0730. The heavy line in these figures indicates where data from the two times is joined.

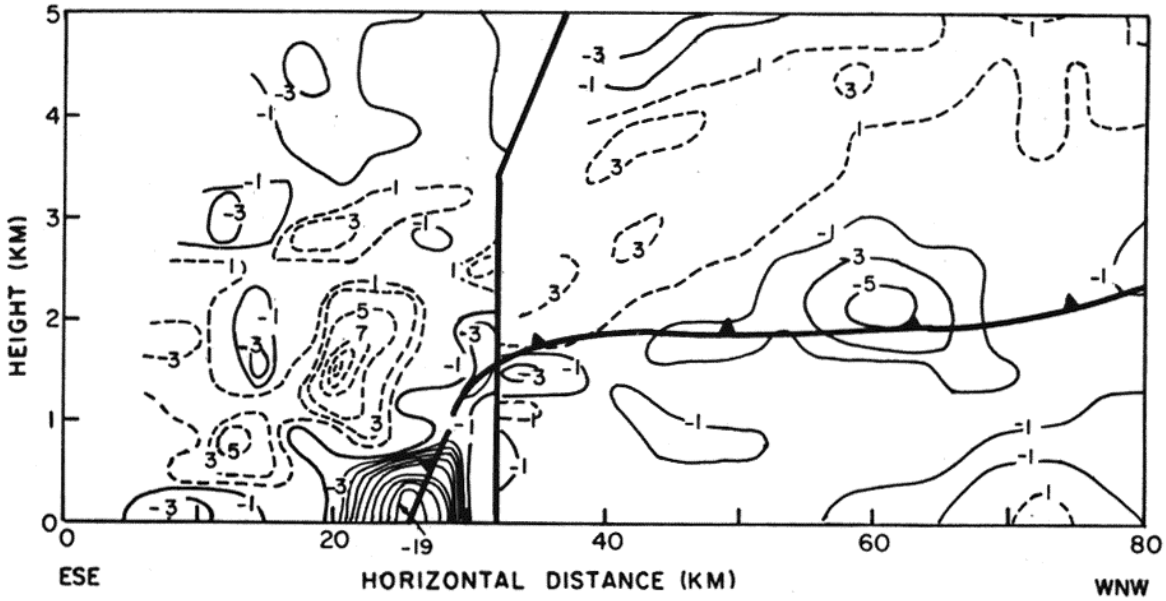

Figure 4: Cross-section through the mesoscale cold-frontal band of cross-front divergence, in units of 10^{-4} s^{-1}. Negative sign indicates convergence.

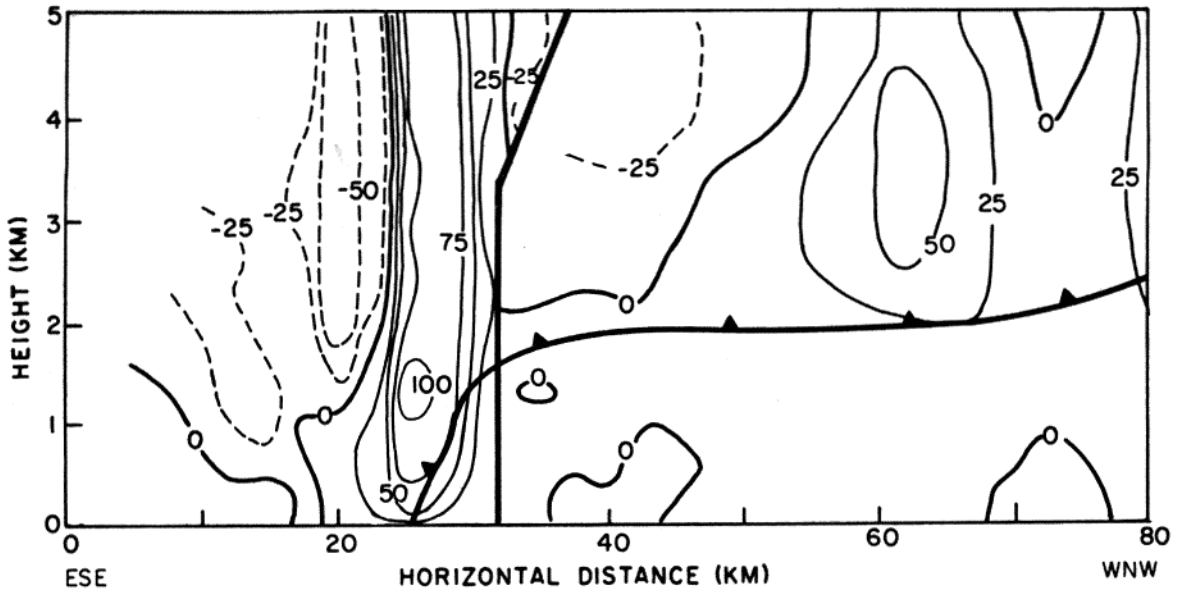

Figure 5: Cross-section through the mesoscale cold-frontal band of vertical velocity, in units of cm s^{-1}. Positive numbers refer to upward velocities.

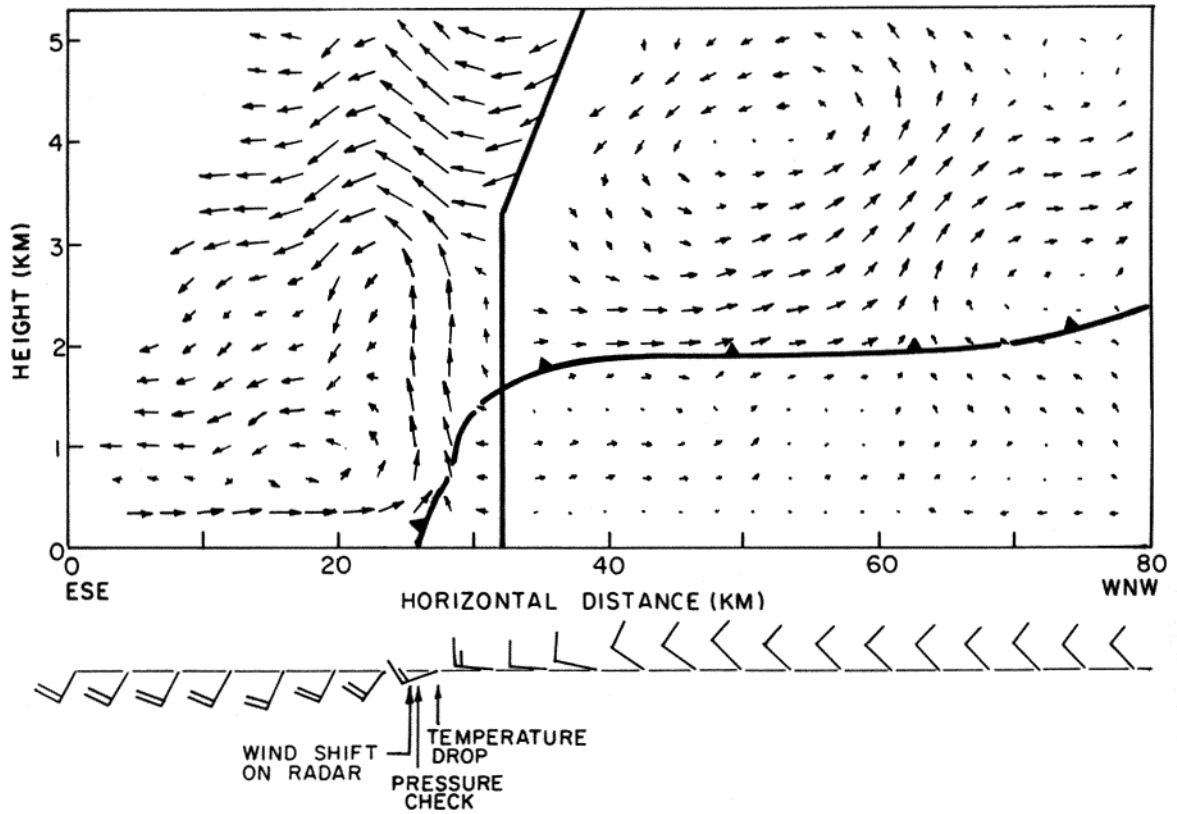

Figure 6: Cross-section through the mesoscale cold-frontal band showing streamflow relative to the front; arrows represent 5 min displacements. The position of the surface windshift seen with the radar is indicated at the bottom; also shown are a wind record and other surface information from the radar site, positioned along the cross-section using the speed of the front to convert time to distance.

A radar bright band, associated with the melting of precipitation particles, appears in Fig. 2 as the band of high reflectivities between altitudes of 2 and 3 km. Between horizontal ranges of 90 and 100 km the layer of high reflectivities behind the front was slightly lower than it was ahead of the front. This agrees with rawinsonde data which show that the 0°C isotherm dropped from 2.5 to 2.3 km across the front.

4. AIRFLOW ASSOCIATED WITH THE COLD FRONT

The flow of air within the cold-frontal band was investigated by applying the equation of continuity to the horizontal component of the measured velocity in a vertical plane oriented perpendicular to the front. Vertical velocities of the air were calculated by assuming that no significant divergence occurred along the front and integrating the cross-front divergence upward in one-third kilometer steps from the surface, where a vertical velocity of zero was assumed. Cross-sections through the mesoscale cold-frontal band of cross-front divergence, vertical velocity, and streamflow relative to the front were produced (Figs. 3-6).

In the region of the band ahead (eastward) of and including the thin line of cellular echoes (B in Fig. 2), the cross-sections in Figs. 4-6 were constructed from velocity data collected at 0700 at an azimuth of 294°, perpendicular to the surface windshift line. For the region of the band behind (westward of) the thin line of cellular echoes, the cross-sections were constructed from velocity data collected at 0730 at an azimuth of 310°. The slight change in azimuth reflects the change in orientation of the cold frontal surface aloft from that at the surface, as evidenced by a change in the orientation of the front and back edges of the cold-frontal band and by a change in orientation of the sub-bands behind the surface front (bands C and D in Fig. 2) as compared with the orientation of sub-bands ahead of and along the front (bands A and B in Fig. 2). The use of the later time for the back portion of the cold-frontal band permits better vertical resolution of that part of the band, as it had then moved closer to the radar site (Fig. 3). The back part of the band at 0730 is joined at the seam indicated in Figs. 3-6 with the cross-section of the forward portion of the band at 0700 to form a continuous cross-section through the cold-frontal band.

The slight change in orientation between the two halves of the cross-section was not significant in the cross-section of reflectivity, and Fig. 2 simply contains data at 0700 at an azimuth of 294°. The change in orientation was of great importance, however, in the velocity cross-sections, particularly in the cross-section of relative streamflow, for the along-front component of the wind was so great that very accurate perpendicularity (within 4°) of the cross-sectional plane to the front was essential for accurate determination of the horizontal component of the flow relative to the front.

The analysis of cross-front divergence, Fig. 4, shows that the strongest convergence (1.9×10^{-3} s^{-1}) occurred in the lowest kilometer at the surface windshift. Somewhat weaker convergence also straddled the cold front aloft. Divergence was present above and ahead of the front, with the strongest divergence occurring at an altitude of 1.5 km immediately ahead of the front and the surface windshift.

The pattern of vertical velocity in the plane of the cross-section (Fig. 5) shows two regions of ascent, one intense and small-scale, related to the convergence associated with the surface windshift, and the other larger-scale and weaker, occurring above the cold-frontal surface aloft.

The circulation associated with the zone of intense lifting just above the surface windshift was dramatic (Fig. 6). Air in the shallow boundary layer in the warm sector moved toward the front, in a relative sense, at speeds of up to 13 m s^{-1}. At the front, this air rose sharply in a column 4 km in width. Vertical velocities up to 1 m s^{-1} occurred in the column (Fig. 5). When this air reached a level of strong wind shear at an altitude of 3 km, it was carried forward; the precipitation in this leg of the circulation may have fallen in the strong sub-band A at the leading edge of the cold-frontal band, ahead of the surface windshift (Fig. 2). A strong downdraft, 4-5 km in width with vertical velocities up to 0.5 m s^{-1}, occurred just ahead of the intense updraft. The base of the downdraft at a height of 1.5 km corresponds with the strong center of divergence seen in Fig. 4. A strong updraft-downdraft pair such as the one seen here is a typical feature of cumulonimbus clouds. The low-level cold frontal windshift thus apparently produces a feature with the properties of a convective cloud of small horizontal scale embedded within the wider cold-frontal precipitation band.

The second region of ascent, that occurring above the cold front aloft, exhibited vertical motions up to a few tens of centimeters per second. These vertical motions were the result of the horizontal convergence straddling the cold front (Fig. 4). It can be seen from Figs. 5 and 6 that the flow above the cold front did not ascend uniformly. The places of relatively stronger ascent were apparently the source of the heavier precipitation in the sub-bands observed behind the surface front.

The results of the analysis of this case agree well with results obtained in previous studies of cold-frontal bands. Browning and Harrold (1970) observed the two contrasting regions of ascent observed here. They noted a small convective-scale downdraft aloft, but it was to the rear of the updraft and not as prominent a feature as in our case. Matejka and Houze (1976) and Matejka *et al.* (1978) present several examples of cold-frontal bands where a strong updraft above the surface front was observed to have the same horizontal scale and the same magnitude as the one described here.

5. CONCLUSIONS

The use of Doppler radar to study the dynamics associated with mesoscale precipitation in extratropical cyclones is a major advance over the use of serial rawinsondes or arrays of rawinsondes. While data from rawinsondes have enabled mesoscale precipitation features to be positioned within the framework of a larger-scale flow (e.g., Houze *et al.*, 1976b), data from Doppler radars provides a highly detailed view of the flow through mesoscale regions of precipitation. Using the precipitation particles as tracers, the velocity of the wind along the beam can be measured with Doppler radar with nearly 100 times the resolution of the best measurements to be expected from ground-launched rawinsondes.

In this paper, we have used Doppler radar data to deduce fields of divergence and vertical velocity and the airflow in the cross-sectional plane through a mesoscale cold-frontal band of precipitation. Two regions of ascent have been identified. At and above the windshift line accompanying the frontal passage at the surface, air from the boundary layer of the warm sector of the cyclone rose sharply, with vertical velocities reaching 1 m s^{-1}, in a column 4 km in width. Associated with this small-scale intense updraft was an intense convective-scale downdraft. Behind the surface front, less vigorous, widespread ascent occurred above the cold front aloft.

The mesoscale cold-frontal band possessed a substructure consisting of several embedded sub-bands. These sub-bands have been associated with details of the airflow pattern.

The results obtained here agree with previous work on the airflow and internal structure of mesoscale cold-frontal bands, and this encourages further use of the CP-3 Doppler radar data collected over several years in the CYCLES PROJECT in deducing the detailed dynamics of mesoscale precipitation bands. In particular, the methods demonstrated in this paper will be applied to the other types of mesoscale bands of precipitation commonly observed in extratropical cyclones (Houze *et al.*, 1976a). Such knowledge of the dynamics of mesoscale precipitation systems in extratropical cyclones is essential to an understanding of the cloud microphysical processes occurring in these storms and may also illuminate mesoscale aspects of frontal dynamics.

ACKNOWLEDGMENTS

We thank Prof. Peter V. Hobbs, Director, and the members of the Cloud Physics Group at the University of Washington who participated in the field program of the CYCLES PROJECT. We also thank Mr. John D. Locatelli for helpful discussions. We appreciate the cooperation of Dr. Robert J. Serafin, Manager, NCAR Field Observing Facility and the help of Mr. James W. Wilson in directing the operation of the NCAR CP-3 radar in the field. This research was sponsored by Grant ATM74-14726-A02 from the Atmospheric Research Section (Meteorology Program) of the National Science Foundation.

REFERENCES

Baynton, H. W., R. J. Serafin, C. L. Frush, G. R. Gray, P. V. Hobbs, R. A. Houze, Jr., and J. D. Locatelli, 1977: Real-time wind measurement in extratropical cyclones by means of Doppler radar. *J. Appl. Meteor.*, *16*, 1022-1028.

Browning, K. A., 1974: Mesoscale structure of rain systems in the British Isles. *J. Meteor. Soc. Japan*, *50*, 314-327.

_____ and T. W. Harrold, 1970: Air motion and precipitation growth at a cold front. *Quart. J. Roy. Meteor. Soc.*, *96*, 369-389.

_____, M. E. Hardman, T. W. Harrold, and C. W. Pardoe, 1973: The structure of rainbands within a mid-latitude depression. *Quart. J. Roy. Meteor. Soc.*, *99*, 215-231.

Gray, G. R., R. J. Serafin, D. Atlas, R. E. Rinehart, and J. J. Boyajian, 1975: Real-time color Doppler radar display. *Bull. Amer. Meteor. Soc.*, *56*, 580-588.

Groginsky, H. L., 1972: Pulse pair estimation of Doppler spectrum parameters. *Preprints 15th Radar Meteor. Conf.*, Amer. Meteor. Soc., Boston, 233-236.

Harrold, T. W. and P. M. Austin, 1974: The structure of precipitation systems -- a review. *J. Rech. Atmos.*, *8*, 41-57.

Houze, R. A., Jr., P. V. Hobbs, K. R. Biswas, and W. M. Davis, 1976a: Mesoscale rainbands in extratropical cyclones. *Mon. Wea. Rev.*, *104*, 868-878.

_____, J. D. Locatelli, and P. V. Hobbs, 1976b: Dynamics and cloud microphysics of the rainbands in an occluded frontal system. *J. Atmos. Sci.*, *33*, 1921-1936.

Lhermitte, R. M., 1972: Real time processing of meteorological Doppler radar signals. *Preprints 15th Radar Meteor. Conf.*, Amer. Meteor. Soc., Boston, 364-369.

Matejka, T. J. and R. A. Houze, Jr., 1976: The internal structure of mesoscale precipitation features in extratropical cyclonic storms. *Preprints 17th Radar Meteor. Conf.*, Amer. Meteor. Soc., Boston, 264-269.

_____, _____, and P. V. Hobbs, 1978: Mesoscale cloud features and their internal structure and dynamics in five extratropical cyclones. Manuscript in preparation.